

Simulating Irregular Source Geometries for Ionian Plumes

W. J. McDoniel^a, D. B. Goldstein^a, P. L. Varghese^a, L. M. Trafton^a,
D. A. Buchta^b, J. Freund^b, and S. W. Kieffer^b

^a*The University of Texas at Austin, Austin, TX 78712*

^b*University of Illinois at Urbana-Champaign, Urbana, IL 61801*

Abstract. Volcanic plumes on Io represent a complex rarefied flow into a near-vacuum in the presence of gravity. A 3D Direct Simulation Monte Carlo (DSMC) method is used to investigate the gas dynamics of such plumes, with a focus on the effects of source geometry on far-field deposition patterns. A rectangular slit and a semicircular half annulus are simulated to illustrate general principles, especially the effects of vent curvature on deposition ring structure. Then two possible models for the giant plume Pele are presented. One is a curved line source corresponding to an IR image of a particularly hot region in the volcano's caldera and the other is a large area source corresponding to the entire caldera. The former is seen to produce the features seen in observations of Pele's ring, but with an error in orientation. The latter corrects the error in orientation, but loses some structure. A hybrid simulation of 3D slit flow is also discussed.

Keywords: Io, Plumes

PACS: 96.12.Jt, 96.25.Xz, 96.30.Ib

INTRODUCTION

Jupiter's moon Io is extremely volcanically active, and its volcanoes give rise to spectacular plumes rising above the surface of the planet and large deposition rings on the ground [1]. Io's atmosphere is thin (several nanobar), and these plumes become rarefied very quickly. Gravity pulls the gas back down to the surface, where it encounters gas on the way up, creating an umbrella-like canopy shock, and a deposition ring where this canopy shock intersects the ground. Interestingly, these plumes and rings are not axially symmetric. In the case of the 300km tall Pele plume, gasdynamic processes result in a huge, red, egg-shaped ring with dark "butterfly wings" inside (Fig. 3b inset). At the same time, close-up images of Io reveal that the sources of these plumes are also irregular. Pele's caldera is shaped something like a peanut, with an IR image further revealing a long, thin, and hot line running through the middle of it (Fig. 3a inset). If the plume material of Pele is produced roughly uniformly from the whole caldera or from just the hot line seen in the IR image, we would have an irregular, curved source, the geometry of which might be expected to account for the shape of the deposition ring and the presence of "butterfly wings".

A study which links the observable features of Io's volcanic plumes to conditions just above the surface would enable a study of the continuum phenomena occurring below and near the surface, which could potentially tell us a great deal about Io's interior. Different source mechanisms would lead to different source geometries, and so we examine the effects of source geometry on overall plume structure and surface deposition patterns. The features of these flows are of broader relevance to rarefied flows involving curved nozzles or combinations of nozzles which form an irregular source region.

MODEL

To investigate the effects of source geometry on plume morphology, we used DSMC [2] to simulate the flow of SO₂ as it rises above the surface of the planet, transitioning from continuum to rarefied flow in the process. The same method has previously been used to simulate plumes evolving from round holes [3]. This planet-scale DSMC code has been developed over a number of years in our group [4, 5, 6].

Although, in reality, complex continuum processes underneath and near the surface determine the specific features of the flow as it expands, we at first simplify matters for this study by supposing that those processes can be modeled as flow out of an input reservoir, using a method adapted from work simulating comet impacts on Earth's moon, which includes collision limiting in the nearly continuous near-field [4]. We specify a vent geometry on the surface of the planet, and then project that geometry downward to obtain the particle reservoir in which molecules are created in each time step. Every time step, molecules are allowed to drift up from the reservoirs and enter the computational domain. At the end of every time step, all molecules remaining below the surface of the planet are deleted.

Pele's deposition ring has a diameter of over 1000km, and the hot line seen in infrared images (Fig. 3a inset) is only about 20km long and is less than 1 km wide. Most of our example simulations are of gas at a vent temperature of 180K and with a vent velocity of 200m/s, which produces smaller plumes having ring diameters of 200km or so. In addition, our simulations are for plumes on the night-side of Pele, where the background atmosphere is essentially nonexistent (on the order of 1 pbar or less). These boundary conditions are chosen simply to speed up the simulations for the purpose of illustration; simulating a full-sized day-side plume is appreciably more costly.

The large difference in scale between the vent and the ring can present difficulties for modeling. Depending on the severity of the scale difference, several methods must be used to resolve the near-field flow while still capturing the far-field. Where this is only a mild problem, such as for the half annulus and the rectangular slit (below), the simulation can be performed on a uniform grid with multiple processors, or with grid stretching. For moderately difficult cases, grid stretching in all three directions is used. For the most extreme cases, the calculation is staged, with a near-field simulation being used as the input condition for a far-field simulation

RESULTS

Four different source geometries were simulated: a rectangular slit, a half-annulus, a line source approximating that seen in the infrared image of Pele's caldera, and a peanut-shaped source approximating the entire caldera. In all cases, except Fig. 3a, molecules were created with a temperature of 180K and an upwards velocity of 200m/s.

Rectangular Slit

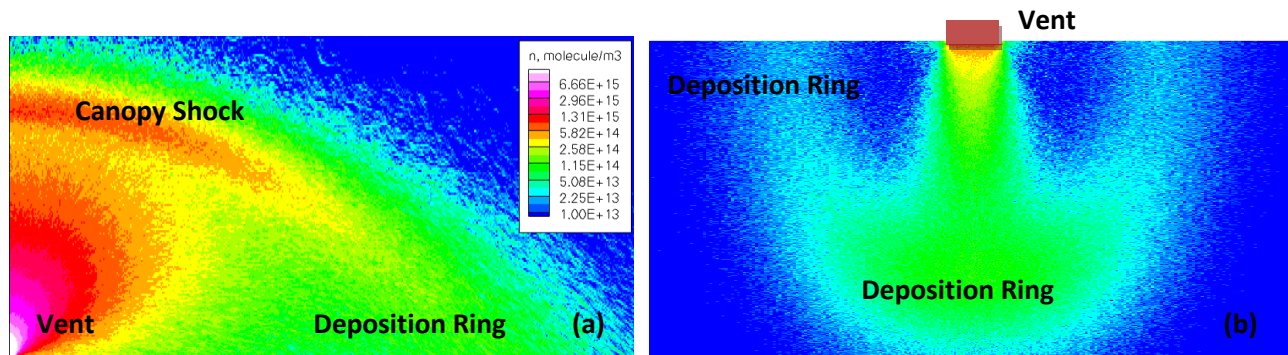


FIGURE 1. Number density contours for the rectangular slit case. A slice through the middle of the plume (a) along the slit's minor axis shows a typical canopy shock seen in many plumes evolving under gravity. A ground-level view of the plume (b) shows a thicker deposition ring along the slit's minor axis, and very low near-ground density near the vent along the major axis.

The first case is a rectangular slit 20km long and 2km wide. This simulation was run on 32 processors, with six million molecules in the processor containing the vent and successively fewer in the remaining processors, and one plane of symmetry was used to cut down on the computational work required. The reservoir number density was $\sim 3 \times 10^{16} \text{m}^{-3}$ and the mean free path just above the vent was $\sim 15\text{m}$. DSMC cells were 150m to a side over the middle of the vent, growing to $\sim 500\text{m}$ in the canopy, resolving the mean free path almost everywhere, except right over the vent.

This case displays many of the basic features that will be of interest later. Initially, the plume expands upwards from its source in a fan of ever-lower gas density. Under the influence of gravity, this large spray collapses back on itself, resulting in a well-defined steady-state canopy shock (Fig. 3a). Where this canopy shock intersects the ground, a deposition ring is formed (Fig. 3b). Because of the irregularity of this vent, the flow-field is not

axisymmetric. Along the major axis of the slit (beyond the end of the slit), the ring's density is lowest, and inside the ring the flow thins out much more quickly. Along the minor axis, the flow is much denser inside the ring, and the ring itself is thicker and even somewhat elongated.

Half Annulus

The second case is a half annular vent 1 km wide and with an inner radius of 7 km. This arbitrary shape was chosen to clearly demonstrate the effects of vent curvature while being feasible on a uniform grid. This simulation was run on 32 processors with several hundred thousand to several million molecules in each processor, and the symmetry of the problem allowed us to simulate only half of the region of interest. The reservoir number density was $5 \times 10^{16} \text{m}^{-3}$. The mean free path just above the vent was $\sim 10 \text{m}$. DSMC cells were 40m to a side for the near-field simulations (slightly under-resolved) and 1 km to a side for the full ring, resolving the deposition ring. The near-vent area of the far-field simulation is seen to match closely with the features of the much better-resolved near-field simulation.

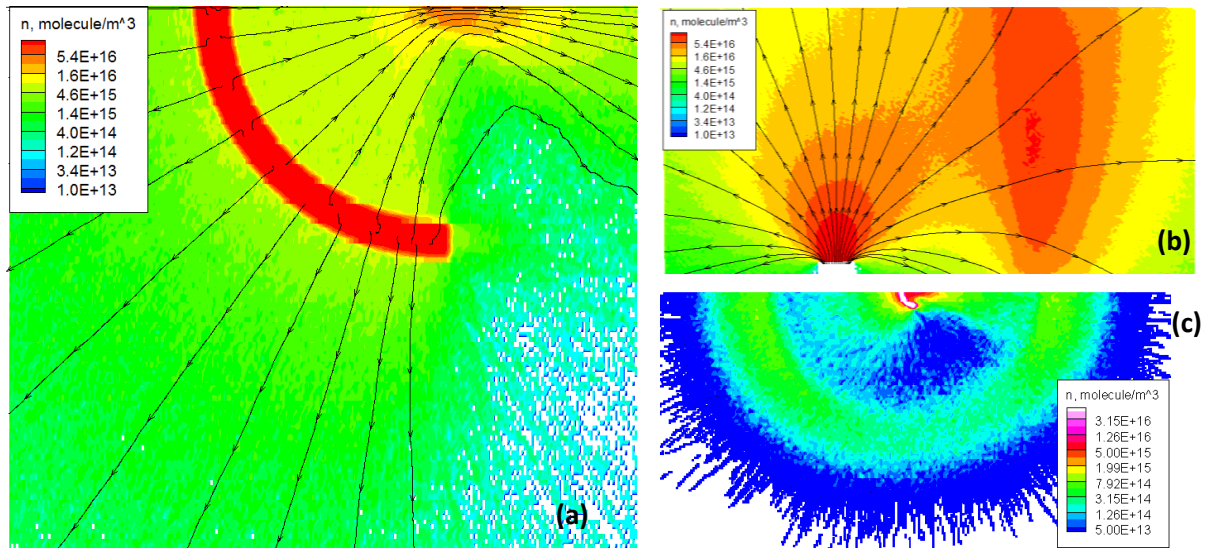


FIGURE 2. Number density contours for the half annulus case. A ground-level view of the near-field (a) with in-plane streamlines (ignoring out-of-plane velocity) makes gas focusing obvious. Note the symmetry plane along the top of the figure. A near-field view of the symmetry plane (b) with streamlines shows the large, standing shock that forms at the focal point of the arc. A far-field ground-level view (c) demonstrates deposition ring elongation along the symmetry axis, with higher densities along the symmetry plane.

Vent curvature has the effect of focusing streamlines on the concave side of the vent. The converging gas, with a Mach number of ~ 2.5 here, shocks, becomes much denser, and turns upward or outward (Fig. 2b) above the center of the “C”. This standing shock creates a large region of high density, which extends further up than the region directly over the vent, and which could conceivably be mistaken for the true source of the plume in an observation. This high-density gas is forced out in a jet, elongating the resulting deposition ring (Fig. 2c) and shifting mass towards the symmetry plane. On the convex side of the vent, radial expansion is observed. There is low density flow in the bottom right corner of Fig. 2a that leads to a low density surface deposition region S/SE of the vent in Fig. 2c. In the end, the ring produced is roughly circular on the convex side, although it becomes less dense away from the symmetry plane, and is elongated on the concave side, producing a roughly egg-shaped ring with one end of the egg sharper than the other. These are important features of real plumes observed on Io, and indicate that vent curvature may play a large role in plume structure.

Curved Line

The third case is a model of the curved line source seen in IR Galileo images of Pele’s caldera (Fig. 3a inset). This source was approximated with 61 small circular discs with 90m radii (and with 100m between each disc center) evenly distributed over the length of the source. To resolve the fine detail at the source, the computation was staged. The near-field was run on 64 processors with several million molecules apiece and a uniform grid with cells 40m to a side. Molecules reaching the boundaries of the near-field were stored and then randomly sampled for the steady-state far-field computation, which was done on 2 processors and a uniform grid with cells 200m to a side. The near-field image of Fig. 3a is for a source at Pele’s vent temperature/velocity conditions – 650K with a vent velocity of 900m/s. The far-field image, however, was only simulated with vent conditions of 180K and 200m/s. The mass flow rate through the vent was held constant from the previous straight slit and half-annulus cases, which yields a vent number density of about $5 \times 10^{18} \text{ m}^{-3}$ and a mean free path of $\sim 0.5\text{m}$ just above the vent. This is under-resolved, but the error should serve to dissipate out gradients (which, nonetheless, remain clear in our simulations).

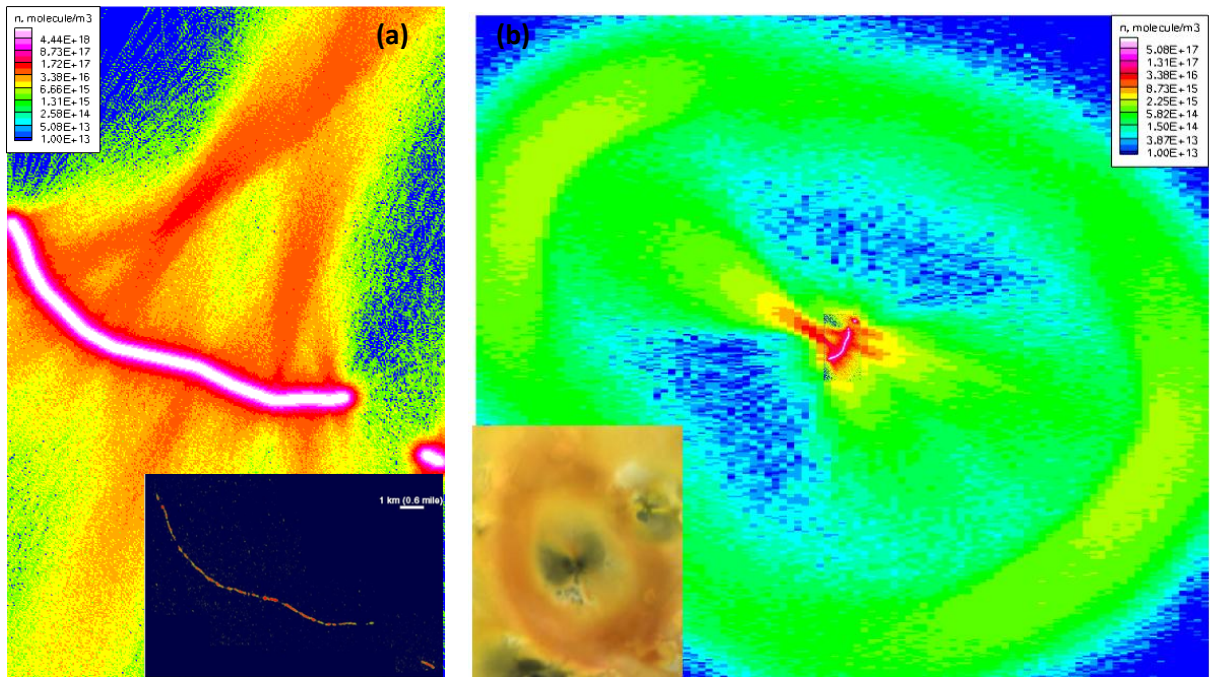


FIGURE 3. Number density contours for the curved line cases. A ground-level view of the hot Pele-class case (a) shows extreme focusing everywhere that the source becomes concave. The far-field ground-level image at 180K, 200m/s conditions (b) shows many of the features seen in Pele’s ring. The inset of Fig. 3a is the infrared Galileo image of Pele’s caldera, and the inset of Fig. 3b is a Galileo image of Pele’s entire red ring. Note that the inset images in the two figures are presented in the geologically correct orientation, but the computational result of Fig. 3b has been rotated for comparison with its inset.

The hot source seen in Fig. 3a demonstrates more extreme focusing in the near-field than that seen in the half annulus case. Jets of concentrated material are sent out of every part of the source that is the least bit concave, and we see the merging of two of these jets in the upper right corner of Fig. 3a. This is significantly more noticeable focusing than seen in the near-field cold case (not shown), and might be expected to produce a more extreme result in the far-field. However, as noted earlier, we do not yet have a far-field calculation for a hot case. The cold far-field case, shown in Fig. 3b, produces an egg-shaped ring which is sharper on one side and blunter on the other. There are two “butterfly wings” of low-density flow inside the ring and perpendicular to the major axis of the egg. This closely matches the overall appearance of Galileo observations of Pele’s ring (inset). However, the simulated orientation appears 90° off (Fig. 3b has been rotated to line up with the observation). As well, although the low-density “butterfly wings” are suggestive, it is believed that the black wings seen in the observation are not merely

the absence of plume material. Rather, black is probably indicative of silicate ash particle deposits. We will shortly be including heavy particle dynamics in our simulations [2] in order to examine this phenomenon.

Peanut

The final case is a peanut-shaped source model of Pele’s entire caldera. This was approximated with 48 rectangular slits of varying length placed next to each other, and was run on 32 processors. A non-uniform processor distribution used 12 processors for the flow directly over the vent, with the remaining 20 flow-field partitions growing larger in longitude. A non-uniform grid was used within each processor, with varying cell sizes in latitude and altitude (cell sizes in longitude were constant within each processor but varied across processors). The cells were smallest ($\sim 150\text{m}$ to a side) on the vent, and grew to $\sim 500\text{m}$ to a side in the far-field. 180K and 200m/s vent conditions were used, and the mass flow rate through the source was held constant from previous simulations, yielding a vent number density of $\sim 2 \times 10^{16}\text{m}^{-3}$.

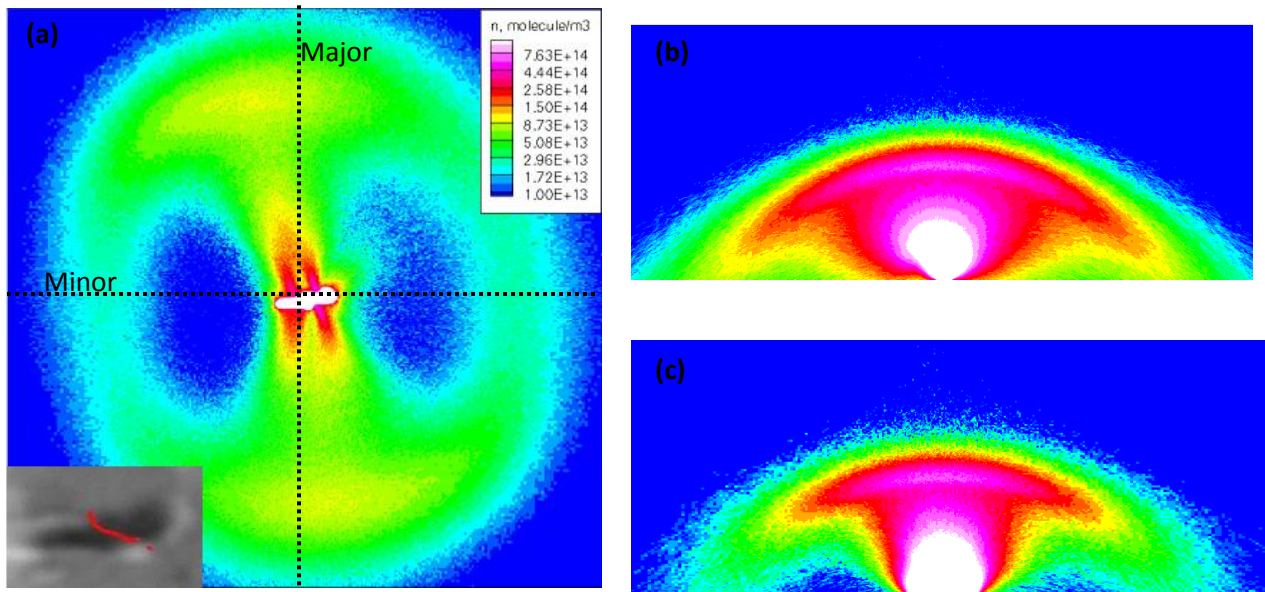


FIGURE 4. Number density contours for the peanut-shaped case. The ground-level far-field image (a) shows the ring and “butterfly wings”. Fig. 4b is a slice through the middle of the plume, along the ring’s major axis, displaying the canopy shock. Fig. 4c is a similar slice along the ring’s minor axis. The inset to Fig. 4a is a Galileo image of Pele’s caldera, with the line source used in the curved line cases picked out in red. The scale is the same on all figures.

The peanut source combines many of the features seen in the rectangular slit and half annulus cases. Although its mean curvature (and thus its focusing effect) is not as extreme as that of the curved line cases of Fig. 3, ring elongation is still observed. The “butterfly wings” of low density are again apparent in Fig. 4a, and the ring is oriented correctly with respect to the observational image shown in the inset to Fig. 3b. However, the “butterfly wings” appear to be too symmetric about the minor axis of the ring. Caused by the same mechanism as those in the rectangular slit case, they do not fan forward as seen in Fig. 3b and its inset. This might be due to small errors in mapping the curvature of the caldera border, but it could also be due to inaccuracies in modeling the plume source as a uniform vent over the caldera. If the actual plume is mostly produced at the edges of the caldera, where lava impinges on frost or where there are cracks in the hardened crust on a magma lake, or is biased towards hotter areas (such as where the line source is seen), then the results might change subtly.

Hybridization

We clearly would like to fully resolve the near field, and ideally our simulations would reach even deep into the crevices from which the plumes develop. The same DSMC method used above can be used in conjunction with a continuum solver to completely model the evolution of realistic plumes where the subsurface and near-surface gas is

in the fully-continuum regime. Instead of subsurface reservoirs, reservoirs along some 3D surface are used, with their properties determined by the output of a continuum solver. While this hybrid solution remains a work in progress, Fig 5 illustrates a very under-resolved example simulation. The UIUC Euler solver was used in the near field of a 10km by 1km slit jet, and data was passed to DSMC on a 50km by 25km plane lying 20km above the vent.

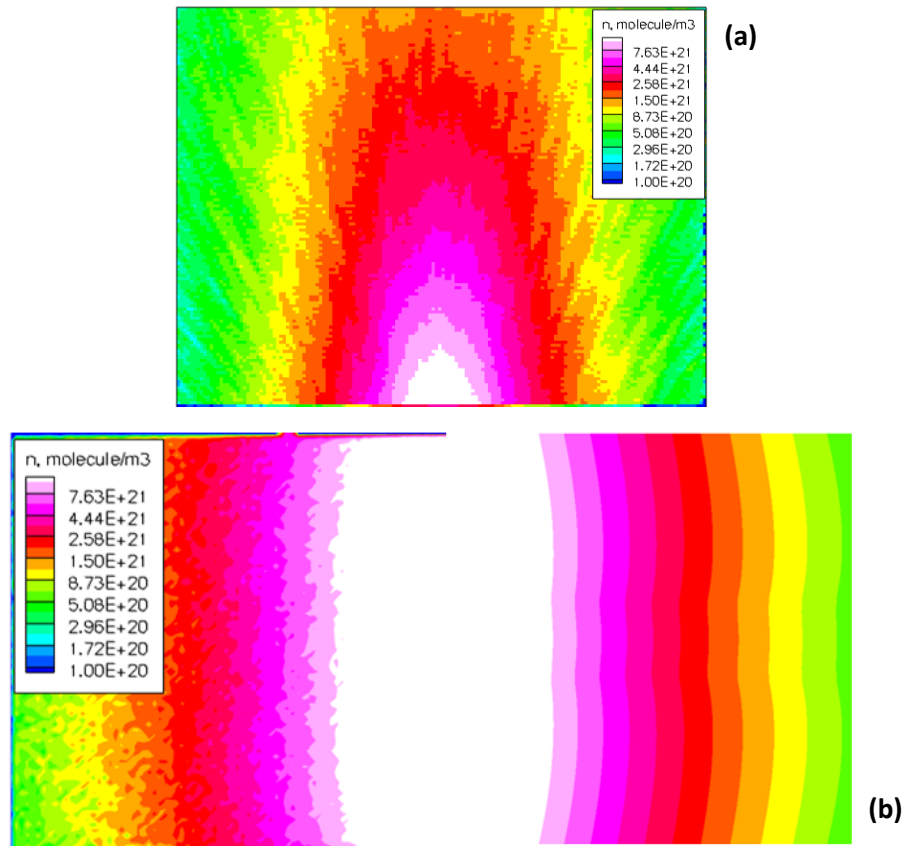


FIGURE 5. Near-field number density contour (a) for a 10km by 1km rectangular slit plume with a vent temperature of 1200K a vent geometry of 450m/s, read into the DSMC domain at an altitude of 20km, and a side-by-side constant-altitude comparison (b) of the DSMC result (left) and the continuum result (right) at 20km.

ACKNOWLEDGMENTS

This work was funded by NASA-PATM grants NNX08AE72G. Large simulations were done on parallel supercomputers at the Texas Advanced Computing Center.

REFERENCES

1. Strom, R.G. and Schneider, N.M. "Volcanic Eruption Plumes on Io". *Satellites of Jupiter* (D. Morrison, Ed.), Univ. of Arizona Press, Tucson (1982).
2. Bird, G.A. *Molecular Gas Dynamics and the Direct Simulation of Gas Flows*. Oxford University Press, London (1994).
3. Zhang, J., Goldstein, D.B., Varghese, P.L., Trafton, L., Moore, C., Miki, K., *Icarus* **172**, 479-502 (2004).
4. Stewart, B.D., Goldstein, D.B., Varghese, P.L., Trafton, L.M., and Moore, C.H., 47th AIAA, #2009-266.
5. Walker, A., Gratiy, S., Goldstein, D., Moore, C., Varghese, P., Trafton, L., Levin, D., Stewart, B., *Icarus* **207**, 409-432 (2010).
6. Austin, J.V. and Goldstein, D.B., *Icarus* **148**, 370-383 (2000).